LOCAL TERNARY PATTERN BASED ON PATH INTEGRAL FOR STEGANALYSIS

Qiuyan Lin, Jiaying Liu and Zongming Guo⋆

Institute of Computer Science and Technology, Peking University, Beijing 100871, China

ABSTRACT

The least significant bit (LSB) matching is a steganographic method which embeds the stego signal into cover images in the spatial domain. However, the stego signal disturbs the correlation of neighboring pixels in cover image and this can be utilized for steganalysis. Local binary pattern (LBP) is an effective image texture descriptor, and it can summarize the correlation of neighboring pixels. In this paper, a LBP-based steganalyzer is proposed to identify the deviations of the correlation violated by the stego noise. Specifically, our paper proposes the local ternary pattern based on path integral (pi-LTP) to enhance the feature discrimination in large-scale pixels. Moreover, a greedy incremental algorithm is utilized in our method to select the optimal subspace of pi-LTP features. Experimental results show our method has a better performance than the state-of-the-art steganalysis methods.

***Index Terms*—** Steganalysis, LSB matching, local ternary pattern (LTP), path integral based LTP (pi-LTP)

1. INTRODUCTION

Nowadays, the classical and practical steganographic algorithms embed the message into the natural images in spatial domain. As the message and the cover images are mutually independent, the impact of steganography is equivalent to embedding the stego noise into images. Least significant bit (LSB) matching is a well-known steganographic method, in which each LSB of the payload pixels is randomly increased or decreased by 1 if it does not match the message bit. This symmetrical embedding procedure makes LSB matching have the advantages of good statistical imperceptibility, high payload and ease of implementation [1, 2].

Steganalysis is an issue of detecting steganography by modelling the stego signal as the addition of noise. One of the first heuristic steganalyzer is based on the histogram characteristic function center of the mass (HCF-COM) [3]. This method is extended to the adjacency HCF-COM by [1] with the calibration technique. Later on, a rather different heuristic method is taken in [4], where the statistical property of the amplitude of local extreme (ALE) is extracted in the gray-level histogram. Some improvements to ALE are by analyzing the amplitudes of local extrema extending to the 2D histogram [5], incorporating the calibration technique into ALE [6], etc. Recently, another heuristic method based on residual images is popular in some literatures. For instance, the subtractive pixel adjacency matrix (SPAM) features based on Markev chains is proposed by [7]; the rich model of the noise components is assembled by forming a union of many image residuals in [8].

Local binary pattern (LBP) [9] is first proposed by Ojala *et al.* as a statistical model of texture analysis. It has been proved to be a powerful tool in other applications of computer vision, such as face analysis [10–12], motion analysis [13] and facial expression recognition [14, 15]. As a local texture descriptor, LBP encodes each pixel of images by comparing it with its neighboring pixels located in a circle, i.e., LBP can summarize the correlation of neighboring pixels. After embedding the stego noise, this correlation will be disturbed because the distribution of stego noise is independent from the cover image. Therefore, it is reasonable to expect the potentials of LBP-based steganalyzers in identifying the deviations of the correlation violated by the stego noise. As for the steganalysis based on LBP, Gui *et al.* [16] propose LBP in rectangularly symmetric neighborhood for steganalysis of LSB matching, and a high detection accuracy shows the advantage of LBP in capturing the pixels correlation. However, at low embedding rate, the detection ability of this method is limited due to lacking the correlation of multi-scale pixels.

In this paper, we propose a new LBP-based steganalytic method which improves the feature discrimination mainly from the following two aspects. First, in the LSB matching, the pixels of cover image are randomly increased or decreased by 1, i.e., the changes of pixels are bidirectional because of the randomly ± 1 noise. Thus, instead of the binary pattern, the local ternary pattern (LTP) [17] is considered to describe the symmetry of stego noise. Second, inspired by the idea of our previously published LBP variant based on path integral (pi-LBP) [18], the correlation of large-scale pixels is captured to enhance the capability of modelling the multi-scale correlation. Unlike LBP which quantizes the difference of one pair of pixels, the multiple pixels along a specific path are filtered and then encoded in pi-LBP. In this way, with flexible choices of paths and filters, the various correlations among the multiple pixels can be directly encoded by pi-LBP. In the synthesis of the above aspects, we propose a LTP variant based on path integral (pi-LTP), which is a combination of LTP and pi-LBP. To further select the optimal subspace of pi-LTP features, a greedy incremental algorithm is utilized for seeking a good trade-off between the feature dimension and discrimination. Finally, the obtained features are trained and classified by ensemble classifiers [19]. Extensive experiments are conducted to show the superiority of our method compared with the state-of-the-art steganalysis methods.

The rest of this paper is organized as follows. The conventional LBP and its variants are described in Section 2. The proposed steganalytic schema based on pi-LTP is introduced in detail in Section 3. The experimental results are shown in Section 4. Finally, we conclude our work in the last section.

2. LBP RELATED WORKS

2.1. LBP

The conventional LBP encodes each image pixel into a binary number according to the signs of the differences between the center pixel c and its adjacent pixels x_p [9]. The operator is laterly generalized to

⋆Corresponding author, e-mail: guozongming@pku.edu.cn

This work was supported by National Natural Science Foundation of China under contract No. 61572052.

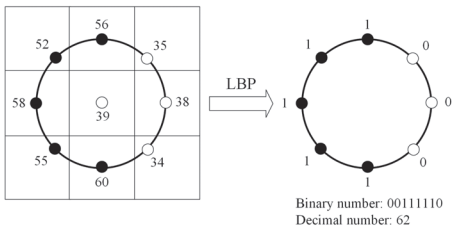

Fig. 1. Example of $\mathrm{LBP}_{8,1}$.

use neighbors with different distances to capture larger-scale structures [20]. Specifically, the neighbors of each pixel are defined as a set of P sampling points located on a R radius circle, which is centered at the pixel c. Then, the sampling points that not fall within the pixels are interpolated using bilinear interpolation. Formally, the generalized LBP can be expressed in a decimal form as

$$\mathrm{LBP}_{P,R} = \sum_{p=0}^{P} s(x_p - c)2^p \tag{1}$$

where the function $s(x)$ is equal to 1 when $x \geq 0$, and 0 otherwise. Taking Fig. 1 as an example, the to-be-labeled pixel value is 39 and its corresponding $\mathrm{LBP}_{8,1}$ is 62.

From the aforementioned definition, there are 2^P different $\mathrm{LBP}_{P,R}$ codes, corresponding to the 2^P binary numbers formed by the P sampling points. However, $\mathrm{LBP}_{P,R}$ codes lack of the robustness against the rotation changes. To remove the rotation effect, the 2^P $\mathrm{LBP}_{P,R}$ codes are then grouped considering the rotational symmetry of natural images. Specifically, a rotation invariant LBP is proposed in [20] as

$$\mathrm{LBP}^{ri}_{P,R} = min\{ROR(\mathrm{LBP}_{P,R}, i)|i = 0, ..., P-1\} \tag{2}$$

where $ROR(x, i)$ represents the circular right shift of bit sequence x by i times (e.g., the result of $ROR(00111100, 3)$ is 10000111), and the superscript "ri" denotes rotation invariant patterns for $\mathrm{LBP}_{P,R}$. After this operator, $\mathrm{LBP}^{ri}_{P,R}$ has totally 36 different values if $P = 8$.

Overall, the LBP feature extraction contains the following three steps. First, each pixel of the image is encoded to the $\mathrm{LBP}_{P,R}$ code as (1). Second, a rule-based strategy like the "ri" strategy is exploited to reduce the feature dimension. Finally, a histogram counting $\mathrm{LBP}^{ri}_{P,R}$ codes is generated as features.

2.2. LTP and LBP based on path integral

To make the feature more discriminative and less sensitive to the noise in uniform regions, the LBP is extended to 3-valued codes called LTP by Tan *et al.* [17]. For LTP operator, an intermediate zone of width $\pm t$ is generated around c. The neighboring pixels in this zone are quantized to 0; the ones above this are quantized to +1 and the ones below it to -1. The function $s(x)$ in (1) is replaced by

$$s'(x,t) = \begin{cases} 1, & x > +t \\ 0, & -t \leq x \leq +t \\ -1, & x < -t \end{cases} \tag{3}$$

In this way, the 2^P valued LBP is extended to the 3^P valued LTP. However, the rotation invariant pattern is not easily applied in the ternary case. For similarity, the coding scheme is split into its positive and negative halves. For example, the ternary code 0011(-1)(-1)00 will be split as the positive code 00110000 and the negative one 00001100. Thus, $\mathrm{LTP}^{\mathrm{ri}}_{\mathrm{P,R}}$ has totally 72 different values if $P = 8$.

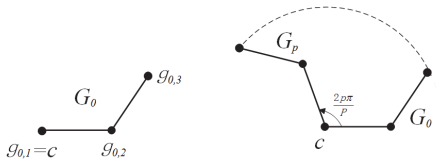

Fig. 2. Illustration of the pi-LBP definition.

The idea of pi-LBP is firstly proposed in [18] to tackle the texture classification issue. In pi-LBP operator, the cross-scale correlation is modelled by quantizing the different scales pixels along a specific path. Specifically, the definition of pi-LBP will be described as following. Supposing that $G_0 = (g_{0,1}, ..., g_{0,k})$ is a specific path, the elements $g_{0,1}, ..., g_{0,k}$ of G_0 are the pixels starting with $g_{0,1} = c$. Then, referring to Fig. 2, the rest paths of $G_p = (g_{p,1}, ..., g_{p,k})$ can be generated by rotating G_0 in an anti-clockwise direction with $(2p\pi)/P$ degree. Specifically, each element $g_{p,i}$ of G_p is the one by rotating $g_{0,i}$ centered at c with $(2p\pi)/P$ degree. Finally, the formal definition of pi-LBP can be expressed by

$$\text{pi–LBP}_{P,G_0,f} = \sum_{p=0}^{P-1} s\left(\sum_{i=1}^{k} f(i)g_{p,i}\right)2^p \tag{4}$$

where $f = (f(1), ..., f(k))$ is a filter that satisfies $\sum_{i=1}^{k} f(i) = 0$ to make it invariant against the monotonic gray-scale changes. One can see from this expression, the pi-LBP depends on three parameters: the number P, the path G_0 and the filter f. With the flexible choices of (P, G_0, f), various types of relationship among neighboring pixels can be considered by pi-LBP.

3. PROPOSED SCHEME

3.1. Rationality of LBP-based steganalyzers

The rationality of LBP-based steganalyzers is illustrated from the following three points. The first point indicates that the steganalyzers are based on the fact that, the stego noise disturbs the high spatial correlation existing in neighboring pixels. In LBP operator, the common texture structures of natural images are represented as their corresponding uniform binary patterns, e.g., the smooth region as 00000000 and the object edge as 11110000. The statistical histograms counting those uniform patterns reflect the spatial correlation of images. However, after embedding the stego noise, the histograms may be changed for the disturbances to the uniform patterns. More specifically, taking the classical Lena image as an example, Fig. 3 shows the distribution differences of the LBP codes between the cover image and the stego image embedded by LSB matching. Here, the bars of histogram with high absolute values are marked by the corresponding binary numbers of LBP. One can see from that, after steganography, the smooth region of cover image may be interpolated into the white spot (e.g. 11111111) and the object edge may be into the irregular form (e.g. 00011101 or 00101111). Based on the deviation of the distribution, we argue that it is reasonable to detect LSB matching using LBP.

The second point indicates that a good model of steganalyzer is usually determined not only by the characteristics of cover images but also by the effects of stego noise. In LSB matching, the embedding noise randomly increases or decreases the pixel values of cover images. Here, the interpolation of pixels is symmetrical for the ± 1 noise. However, the conventional LBP is not strictly symmetrical for the rough definition of $s(x)$ at $x = 0$ in (1). Thus, instead of the binary pattern, the ternary pattern of LTP [17] is considered in our steganalyzer to capture the symmetrical changes of LSB matching. For

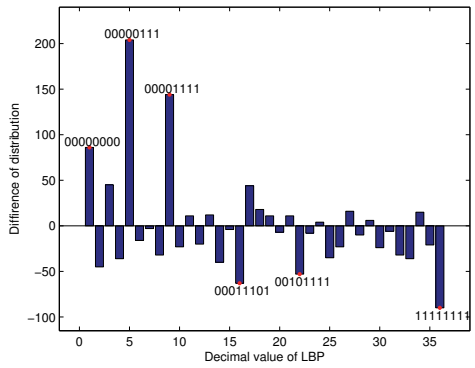

Fig. 3. Histogram difference of the 36 dimensional $\text{LBP}^{ri}_{P,R}$ between the cover image and the stego image embedded by LSB matching at embedding rate 0.1.

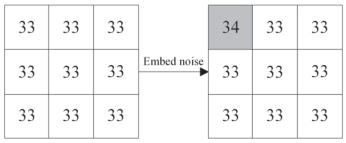

Fig. 4. The smooth region of the cover image and the stego image.

example, one smooth region of Fig. 4 may be modified by steganography, where the original and modified center pixels are represented as the same LBP code (00000000) but the different positive codes of LTP (00000000 and 00010000). In addition, considering the rotational symmetry of natural images, the "ri" strategy is adopted for the feature dimension reduction.

The third point indicates that the rich features of steganalyzer need to capture the various types of relationship among neighboring pixels. In pi-LBP, the correlation of large-scale pixels is captured to enhance the capacity of modelling the multi-scale noise. Unlike LBP which only quantizes the difference of two adjacent pixels, the multi-pixels along a specific path are filtered and then encoded in pi-LBP. In this way, with flexible choices of paths and filters, the various correlation can be directly encoded by pi-LBP to improve the discrimination of features.

Based on the above analysis, we argue that it is reasonable to detect LSB matching considering the combined features of LTP and pi-LBP (called pi-LTP).

3.2. pi-LTP in the square rotation

In pi-LBP defined by [18], the sampling points of paths that do not fall within the pixels are interpolated using bilinear interpolation. However, the modification of each pixel is at most 1 after LSB matching, so the bilinear interpolation may lead to the interpolation less obvious. Hence, instead of pi-LBP in the circumferential rotation, we propose a new pi-LBP in the square rotation.

We first give the definition of pi-LBP in the square rotation. Similarly as the left figure of Fig. 2, $G_0 = (g_{0,1}, ..., g_{0,k})$ is a path of the image, where the first element $g_{0,1}$ may not be the pixel c. For each element $g_{0,i}$ of G_0, taking c as the center, one and the only one square S_i can be determined and the length of its sides is labelled as l_i. Then, referring to Fig. 5, along the sides of rectangle R_i, we move $g_{0,i}$ with the step of $4l_ip/P$ pixels in length to get the position of $g_{p,i}$ of G_p. That is to say, the G_p is obtained by rotating each element in a square track. So the proposed method is called pi-LBP

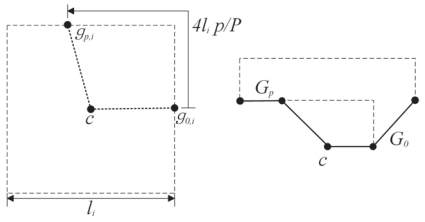

Fig. 5. Illustration of the pi-LBP in the rectangular rotation.

in the square rotation. It should be noted that, if the elements of G_0 are right in the center of pixels, all elements of the other paths G_p will also exactly locate in the center.

As illustrated above, we also adopt the ternary pattern to the pi-LBP, and the formal definition of pi-LTP can be expressed by

$$\text{pi–LTP}_{P,G_0,f,t} = \sum_{p=0}^{P-1} s'\left(\sum_{i=1}^{k} f(i)g_{p,i}, t\right)2^p \qquad (5)$$

where the function $s'(x,t)$ is defined in (3). Same as the conventional LBP, we also adopt the "ri" strategy in our method ($\text{pi–LTP}^{ri}_{P,G_0,f,t}$) for feature dimension reduction.

3.3. The greedy incremental algorithm

The proposed pi-LTP depends on four parameters: the number P, the path G_0, the filter f and the value t. In this paper, we take $P = 8$ like most LBP variants and $t \in \{0, 1\}$ that will be discussed in the experimental section. The remaining parameters of G_0 and f are firstly enumerated respectively. Then the pair of them (G_0, f) is selected by a greedy strategy. To be specific, the filter f selects some widely used high-pass filters listed in Table 1 for the sake of simplicity. And the path G_0 enumerates the combinations of the successive pixels starting from the center pixel or its right neighboring pixel. As for selecting the pair of (G_0, f), we propose a greedy incremental algorithm to get a good trade-off between the feature dimensionality and discrimination. In this algorithm, the local optimal parameter (G_0^*, f^*) whose prediction error $localE$ is minimum, will be prioritized by our final features fea. Then, if the $localE$ is smaller than the global prediction error $globalE$, the features of $\text{pi-LTP}^{ri}_{P,G_0^*,f^*,t}$ with $P = 8$ and $t = 0, 1$ will be appended to the features fea. The following pseudocode summarizes the algorithm:

Algorithm 1 The greedy incremental algorithm

Initialize $fea \leftarrow \{\}$, $globalE \leftarrow 1$.
while True **do**
  # Get the local optimal parameter (G_0^*, f^*).
  $localE \leftarrow 1$
  for Each filter f and path G_0 **do**
    Train and test to obtain the error E for the feature $\{fea, \text{pi–LTP}^{ri}_{8,G_0,f,0}, \text{pi–LTP}^{ri}_{8,G_0,f,1}\}$.
    if $E < localE$ **then**
      $localE \leftarrow E$, $(G_0^*, f^*) \leftarrow (G_0, f)$.
    end if
  end for
  # Update the optimal parameter fea.
  if $localE < globalE$ **then**
    $globalE \leftarrow localE$.
    $fea \leftarrow \{fea, \text{pi–LTP}^{ri}_{8,G_0^*,f^*,0}, \text{pi–LTP}^{ri}_{8,G_0^*,f^*,1}\}$.
  else
    Break the loop.
  end if
end while

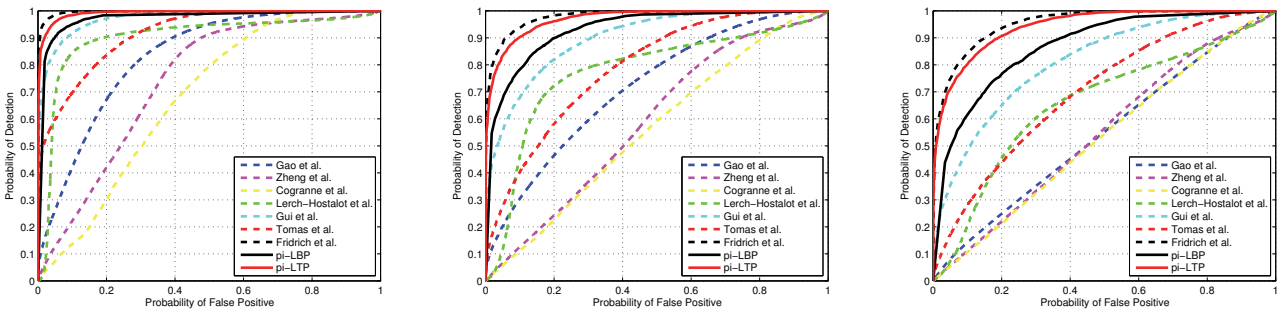

(a) $q = 0.30$ (b) $q = 0.10$ (c) $q = 0.05$

Fig. 6. Comparison of ROC curves between the proposed method and the methods of Gao *et al.* [6], Zheng *et al.* [21], Cogranne *et al.* [22], Lerch-Hostalot *et al.* [23], Tomas *et al.* [7], Gui *et al.* [16], Fridrich *et al.* [8], for the 10,000 gray-scale images of Bossbase 1.01.

Table 1. Filters.

$k = 2$	$(-1, 1)$
$k = 3$	$(-3, 2, 1)$, $(-2, 1, 1)$, $(1, -2, 1)$, $(1, 1, -2)$
$k = 4$	$(-4, 2, 1, 1)$, $(-3, 1, 1, 1)$ $(1, -1, -1, 1)$, $(1, -1, 1, -1)$, $(1, 1, -1, -1)$

Table 2. Comparison of AUC for LTP for different t at embedding rates of 0.30, 0.10 and 0.05 bpp.

t	FD	$q = 0.30$	$q = 0.10$	$q = 0.05$
0	72	0.916	0.802	0.714
1	72	0.763	0.633	0.573
2	72	0.653	0.555	0.527
0,1	144	0.942	0.886	0.830
0,1,2	216	0.954	0.905	0.853

4. EXPERIMENTAL RESULTS

Our experiments are set and conducted on the BOSSbase 1.01 database [24], which contains 10,000 gray-scale images of size 512 $\times$ 512. To evaluate the performances of the proposed feature sets, we embed the images by the LSB matching with the embedding rates of 0.30, 0.10 and 0.05 bpp. As for the parameters of pi-LTP$^{ri}_{P,G_0^*,f^*,t}$, two parameters are taken into consideration. The value of t is chosen from {0, 1, 2} and the pair of (G_0, f) is obtained by training cover images and stego images at the embedding rate 0.10 with the Algorithm 1. Finally, we compare our pi-LBP and pi-LTP steganalyzers to the prior state-of-the-art methods. Here, the measures under the receiver operating characteristic (ROC) curve and the area under curve (AUC) are used to evaluate the performances of the steganalyzers. For consistency, the features of all compared methods are trained and classified using ensemble classifiers [19], in 10-fold cross validation mode.

Above all, the comparison of AUC of LTP with different t is shown in Table 2, where "FD" means the feature dimension. One can see from that, the AUC for LTP when $t = 2$ is mostly close to 0.5 that corresponds to random guessing. That is because the modification of each pixel value after embedding is at most 1. So, we choose $t = 0$ and $t = 1$ in our steganalyzer for the trade-off between detection accuracy and feature dimension. Besides, based on our experiment, the Algorithm 1 totally obtains 27 pairs of (G_0, f). Therefore, the feature dimension of pi-LBP is 27 * 2 * 36 = 1944 in pi-LBP and the one of pi-LTP is 27 * 2 * 72 = 3888.

Further experimental results of ROC for different steganalyzers are shown in Fig. 6. Our method is evaluated by comparing with seven targeted steganalyzers of Gao *et al.* [6], Zheng *et al.* [21], Cogranne *et al.* [22], Lerch-Hostalot *et al.* [23], Tomas *et al.* [7], Gui *et al.* [16] and Fridrich *et al.* [8]. It should be mentioned that the last steganalyzer [8], called *rich model*, is the state-of-the-art method with feature dimension 34671 and has the highest detection accuracy we have known so far.

One can see from Fig. 6 that: 1) Except for the rich model, our method pi-LBP (black solid curve) is significantly superior to the other methods at all embedding rates, proving the effectiveness of detecting LSB matching by pi-LBP. 2) Our improved method pi-LTP (red solid curve) further improves the case of pi-LBP and its advantage over other methods [6, 7, 16, 21–23] is more obvious. 3) The rich model in [8], is an effective steganalyzer with the highest detection accuracy we have known so far. This method is slightly better than pi-LTP. However, the dimensionality of rich model is 34671 while pi-LTP only has 3888 dimension features. 4) At the embedding rate of 0.30, 0.10 and 0.05 bpp, the AUCs of the pi-LTP are 0.992, 0.970 and 0.941 respectively, while the ones of rich model are 0.996, 0.979 and 0.956 respectively. This means our method has a competitive ability of detection at small embedding rates with lower feature dimension. In conclusion, the experimental results show that our method has a good trade-off between the detection accuracy and the feature dimension. Besides, it can effectively detect LSB matching and is better than some state-of-the-art targeted steganalyzers.

5. CONCLUSION AND RELATION TO PRIOR ART

Towards the specific disturbances caused by steganography, in this paper, the combined feature of LTP and pi-LBP is proposed to extract the critical dissimilarities between the cover and stego images. With diverse and flexible parameters, the proposed pi-LTP describes the dissimilarities from multiple angles. To further select the optimal subspace of pi-LTP features, a greedy incremental algorithm is utilized to achieve a good trade-off between the feature dimensionality and discrimination. Experimental results on the BOSSbase 1.01 database verify the superiority of our method.

To our best knowledge, the steganalysis of LSB matching based on LBP has not been studied so far. But the finite research results have shown the great potential of LBP-based features for steganalysis. In the further, we would like to investigate a larger subspace of pi-LTP feature, where the major challenge would be dealing with high feature dimensionality.

6. REFERENCES

[1] A. D. Ker, "Steganalysis of LSB matching in grayscale images," *IEEE Signal Process. Lett.*, vol. 12, no. 6, pp. 441–444, Jun. 2005.

[2] X. Li, B. Yang, D. Cheng, and T. Zeng, "A generalization of LSB matching," *IEEE Signal Process. Lett.*, vol. 16, no. 2, pp. 69–72, Feb. 2009.

[3] J. J. Harmsen and W. A. Pearlman, "Steganalysis of additive noise modelable information hiding," in *Security and Watermarking of Multimedia Contents V*, 2003, vol. 5020 of *SPIE*, pp. 131–142.

[4] J. Zhang, I. J. Cox, and G. Doërr, "Steganalysis for LSB matching in images with high-frequency noise," in *Proc. IEEE MMSP*, 2007, pp. 385–388.

[5] G. Cancelli, G. Doërr, I. J. Cox, and M. Barni, "Detection of +-1 LSB steganography based on the amplitude of histogram local extrema," in *Proc. IEEE ICIP*, 2008, pp. 1288–1291.

[6] Y. Gao, X. Li, B. Yang, and Y. Lu, "Detecting LSB matching by characterizing the amplitude of histogram," in *Proc. IEEE ICASSP*, 2009, pp. 1505–1508.

[7] T. Pevnỳ, P. Bas, and J. Fridrich, "Steganalysis by subtractive pixel adjacency matrix," *IEEE Trans. Inf. Forens. Security*, vol. 5, no. 2, pp. 215–224, Jun. 2010.

[8] J. Fridrich and J. Kodovskỳ, "Rich models for steganalysis of digital images," *IEEE Trans. Inf. Forens. Security*, vol. 7, no. 3, pp. 868–882, Jun. 2012.

[9] T. Ojala, M. Pietikäinen, and D. Harwood, "A comparative study of texture measures with classification based on featured distributions," *Pattern Recognition*, vol. 29, no. 1, pp. 51–59, Jan. 1996.

[10] T. Ahonen, A. Hadid, and M. Pietikäinen, "Face recognition with local binary patterns," in *Proc. ECCV*. 2004.

[11] L. Zhang, R. Chu, S. Xiang, S. Liao, and S. Z. Li, "Face detection based on multi-block LBP representation," in *Proc. ICB*, 2007.

[12] Z. Chai, Y. Zhang, Z. Du, and D. Wang, "Learning flexible block based local binary patterns for unconstrained face detection," in *Proc. IEEE ICME*, 2014.

[13] M. Heikkilä and M. Pietikäinen, "A texture-based method for modeling the background and detecting moving objects," *IEEE Trans. Pattern Anal. Mach. Intell.*, vol. 28, no. 4, pp. 657–662, Apr. 2006.

[14] G. Zhao and M. Pietikäinen, "Dynamic texture recognition using local binary patterns with an application to facial expressions," *IEEE Trans. Pattern Anal. Mach. Intell.*, vol. 29, no. 6, pp. 915–928, Jun. 2007.

[15] C. Shan, S. Gong, and P. W. McOwan, "Facial expression recognition based on local binary patterns: A comprehensive study," *Image and Vision Computing*, vol. 27, no. 6, pp. 803–816, May 2009.

[16] X. Gui, X. Li, and B. Yang, "Steganalysis of lsb matching based on local binary patterns," in *Proc. IEEE IIH-MSP*, 2014.

[17] X. Tan and B. Triggs, "Enhanced local texture feature sets for face recognition under difficult lighting conditions," *IEEE Trans. Image Process.*, vol. 19, no. 6, pp. 1635–1650, Jun. 2010.

[18] Q. Lin and W. Q, "Multi-scale local binary patterns based on path integral for texture classification," in *Proc. IEEE ICIP*, 2015.

[19] J. Kodovskỳ and J. Fridrich, "Ensemble classifiers for steganalysis of digital media," *IEEE Trans. Inf. Forens. Security*, vol. 7, no. 2, pp. 432–444, Apr. 2012.

[20] T. Ojala, M. Pietikäinen, and T. Mäenpää, "Multiresolution gray-scale and rotation invariant texture classification with local binary patterns," *IEEE Trans. Pattern Anal. Mach. Intell.*, vol. 24, no. 7, pp. 971–987, Jul. 2002.

[21] E. Zheng, X. Ping, T. Zhang, and G. Xiong, "Steganalysis of LSB matching based on local variance histogram," in *Proc. IEEE ICIP*, 2010.

[22] R. Cogranne and F. Retraint, "An asymptotically uniformly most powerful test for LSB matching detection," *IEEE Trans. Inf. Forens. Security*, vol. 8, no. 3, pp. 464–476, Mar. 2013.

[23] D. Lerch-Hostalot and D. Megias, "LSB matching steganalysis based on patterns of pixel differences and random embedding," *Computers & Security*, vol. 32, pp. 192–206, Feb. 2013.

[24] T. Filler, T. Pevny, and P. Bas, "Break our steganography system," Jul. 2010, [Online]. http://boss.gipsa-lab.grenoble-inp.fr.